

## 10.4 A 23-to-29GHz Differentially Tuned Varactorless VCO in 0.13 $\mu$ m CMOS

KaChun Kwok<sup>1</sup>, John R. Long<sup>1</sup>, John J. Pekarik<sup>2</sup>

<sup>1</sup>Delft University of Technology, Delft, The Netherlands

<sup>2</sup>IBM Microelectronics, Burlington, VT

Broadband wireless applications such as ultra-wideband communication and radar sensors require RF circuits operating over a range greater than 5% of their nominal operating frequency. For a varactor-tuned voltage-controlled oscillator (VCO), the fixed parasitic capacitances from the negative resistance cell, output buffer, and tank inductor limit the tunable range of the tank capacitance [1][2][3]. In addition, the capacitance tuning ratio ( $C_{\max}/C_{\min}$ ) of a conventional on-chip varactor is typically less than 3, which constrains the tuning range of a monolithic implementation. When additional components are added to correct for process variations, their parasitic capacitances also reduce the operating frequency and tuning range. However, VCOs with a wide tuning range at low-GHz frequencies have been implemented using narrowband oscillators with a capacitor array reconfigured via FET switches. Aside from susceptibility to process variations and difficulties encountered migrating such a design to higher frequencies, other disadvantages of this approach are discontinuities in the tuning curve and slow tuning speed.

This paper describes a (nominally) 26GHz varactorless VCO with 6GHz (24%) continuous tuning range. The circuit may be tuned differentially for rejection of common-mode interferences (e.g., supply noise) in a system-on-chip application such as radar, and it is monotonic when continuously swept from low to high frequency. It requires no tuning capacitors (i.e., varactors). The principle of the tuning scheme is illustrated in Fig. 10.4.1. For an ideal transconductor ( $G_m$ ) with terminal voltage  $V_{g2}$  and controlling voltage  $V_{g1}$ , the impedance seen looking into node A is  $Z_e = V_{g2}/(G_m V_{g1})$ . It can be shown that the wideband tank of Fig. 10.4.1 (inductors  $L_1$ ,  $L_2$  and  $L_3$ , capacitor  $C_1$ , and resistor  $R_1$ ) provides nearly 90° phase shift between  $V_{g2}$  and  $V_{g1}$  at 30GHz. Therefore, impedance  $Z_e$  is a tunable inductance that varies with the value of  $G_m$ . The responses of  $V_{g2}/V_{g1}$  for different values of  $R_1$  as a function of frequency are shown in Fig. 10.4.2. As seen from the figure, a small value of  $R_1$  is desirable in order to maintain a flat magnitude response and phase shift close to 90° across the widest frequency range. However, a small value of  $R_1$  shunting inductor  $L_2$  lowers the tank quality factor (Q). In the final design,  $R_1$  is set at 30 $\Omega$  which gives a minimum tank Q of 2.7 (at 26GHz) across the tuning range.

A simplified schematic of the fully symmetric transconductance-tuned VCO is shown in Fig. 10.4.3. Inductors  $L_1$ ,  $L_2$ , and  $L_3$  from Fig. 10.4.2 form an equivalent T-model for the on-chip transformer ( $T_1$  or  $T_2$ ) used in the tank. Each of the transformers is implemented as single-turn interwound coils of 4 $\mu$ m aluminum thick top metal with a coupling (k) factor of 0.45 and an outside dimension of 120 $\mu$ m per side. A negative resistance cell is implemented using cross-coupled differential pair  $M_1$ ,  $M_2$ . Capacitor  $C_1$  (from Fig. 10.4.2) is provided by the gate capacitance of  $M_7$  and  $M_8$ , which simultaneously implement an open-drain buffer capable of driving a 50 $\Omega$  load for measurement. Differential tuning of the frequency rejects any common-mode noise seen by the tuning nodes present from power supply noise, substrate coupling effects, etc., thereby reducing common-mode induced phase noise. The differential transconductor ( $M_3$ - $M_6$ ) is tunable for both positive and negative values of  $G_m$  and uses tuning current sources  $I_{\text{tune}+}$  and  $I_{\text{tune}-}$ . With  $I_{\text{tune}+}$  set equal to  $I_{\text{tune}-}$ , signal currents from differential pairs  $M_3$ ,  $M_4$  and  $M_5$ ,  $M_6$  cancel resulting in an effective

$G_m$  of zero. With  $I_{\text{tune}+} = 0$ ,  $M_5$  and  $M_6$  are turned off, and  $G_m$  reaches its maximum positive value. Similarly, for  $I_{\text{tune}-} = 0$ ,  $G_m$  reaches its maximum negative value when  $M_3$  and  $M_4$  are turned off. The tuning currents are provided by a resistively degenerated differential pair (not shown in Fig. 10.4.3). A pair of single-ended 0 to 1.5V (max) input voltages (equivalent to  $\pm 1.5$ V differential) provides frequency tuning.

The tank design is centered at 26.3GHz, and the simulated tank impedance ( $Z_{\text{tank}}$ ) as a function of tuning voltage is shown in Fig. 10.4.4. The 0°-phase-shift point for  $Z_{\text{tank}}$  changes from 23 to 31GHz as the differential tuning voltage varies by  $\pm 1.6$ V. The magnitude of  $Z_{\text{tank}}$  is minimum for  $V_{\text{tune}}$  of 0V and gives an equivalent Q factor of 2.4 (as defined by the -3dB bandwidth).

Frequency modulation of a VCO in a radar application (e.g., frequency chirping) enhances resolution and resilience to multi-path interference. By applying a -40dBm sinusoidal with frequency  $\omega_m$  to the differential tuning nodes, the VCO is narrowband frequency modulated with two sidebands offsetted from the carrier by  $\omega_m$ . The measured modulation bandwidth defined by the -3dB frequency of the sidebands is 90MHz. This makes the VCO suitable for a wide range of frequency modulation schemes in radar and communications.

The VCO test circuit is implemented in a 0.13 $\mu$ m mixed-signal CMOS technology [4], which has a substrate resistivity of 10 $\Omega$ -cm. Differential-mode tuning (see Fig. 10.4.5) is continuous and monotonic from 23.2 to 29.4GHz (23.6% range). By comparison, the common-mode tuning range is 26.6 to 27.5GHz (just 3.3%), highlighting the effectiveness of the differential scheme. Average single-ended output power delivered to a 50 $\Omega$  load across the entire tuning range is approximately -11dBm (dashed curve in Fig. 10.4.5). The measured output spectrum at 26.6GHz is shown in Fig. 10.4.6. Phase noise measured at the mid-point of the tuning curve is -96.2dBc/Hz at 3MHz offset, which is suitable for radar applications [5]. Total power consumption is 43mW (including 6.5mW from the 50 $\Omega$  buffer) from a single 1.2V supply. The 1 $\times$ 1.4mm<sup>2</sup> test chip (including bondpads; 0.3 $\times$ 0.4mm<sup>2</sup> for the VCO core) is shown in Fig. 10.4.7.

### References:

- [1] M. Tiebout, H. Wohlmuth, and W. Simbuerger, "A 1V 51GHz Fully-Integrated VCO in 0.12 $\mu$ m CMOS," *ISSCC Dig. Tech. Papers*, pp. 300-301, Feb., 2002.
- [2] A. Ng, G. Leung, K. Kwok, L. Leung, and H. Luong, "A 1V 24GHz 17.5mW PLL in 0.18 $\mu$ m CMOS," *ISSCC Dig. Tech. Papers*, pp. 158-159, Feb., 2005.
- [3] S. Yun, S. Shin, H. Choi, and S. Lee, "A 1mW Current-Reuse CMOS Differential LC-VCO with Low Phase Noise," *ISSCC Dig. Tech. Papers*, pp. 540-541, Feb., 2005.
- [4] IBM Corp., "Foundry Technologies 130-nm CMOS and RF CMOS," *IBM Product Brief*, 2003.
- [5] J. Mueller, T. Grave, H. Siweris, et al., "A GaAs HEMT MMIC Chip Set for Automotive Radar Systems Fabricated by Optical Stepper Lithography," *IEEE J. Solid State Circuits*, vol. 32, pp. 1342-1349, Sept., 1997.

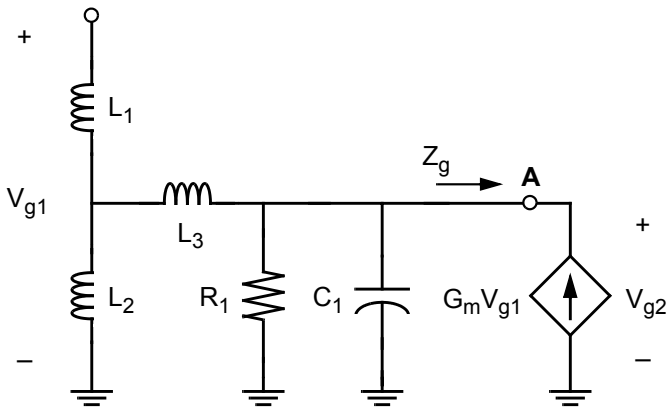


Figure 10.4.1: Principle of transconductance (i.e., varactorless) frequency tuning.

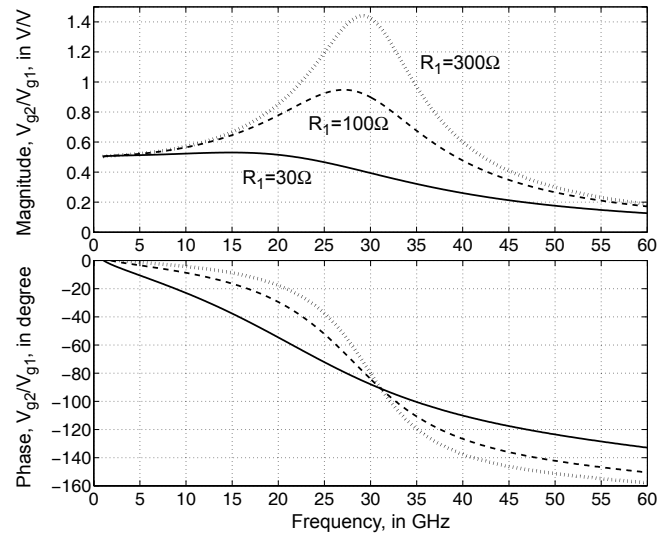
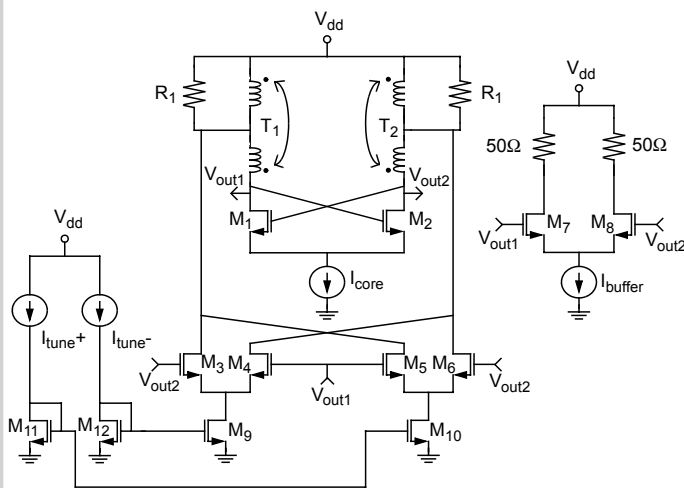
Figure 10.4.2: Amplitude and phase responses of  $V_{g2}/V_{g1}$  for different  $R_1$  values.

Figure 10.4.3: Simplified schematic of the transconductance-tuned VCO.

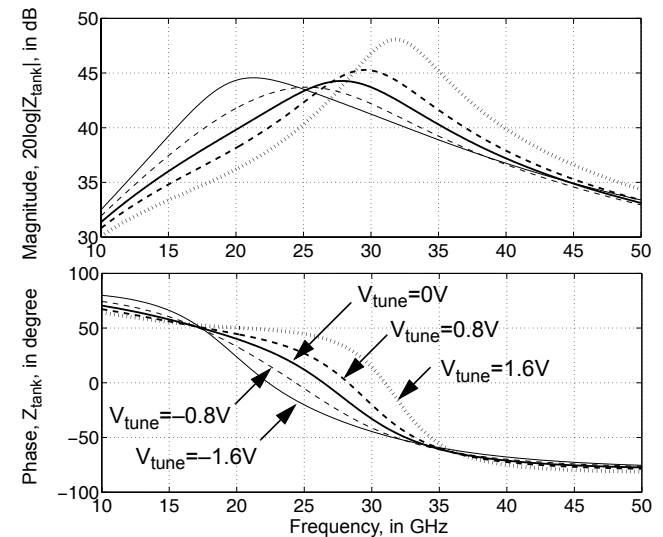
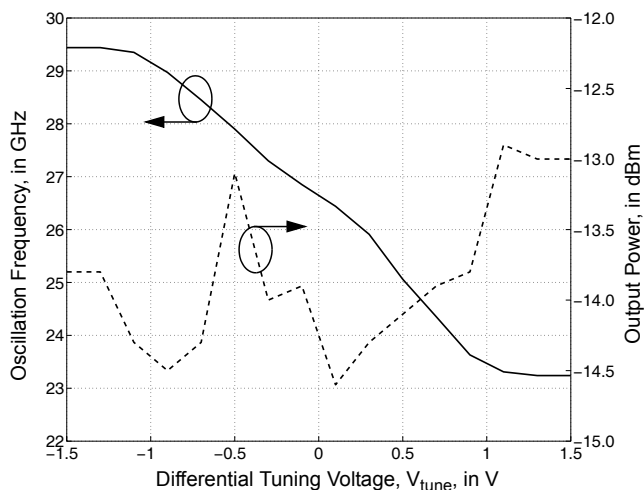
Figure 10.4.4: Simulated tank impedance versus frequency with  $\pm 1.6$ V tuning voltage.

Figure 10.4.5: Measured output frequency and power versus differential tuning voltage.

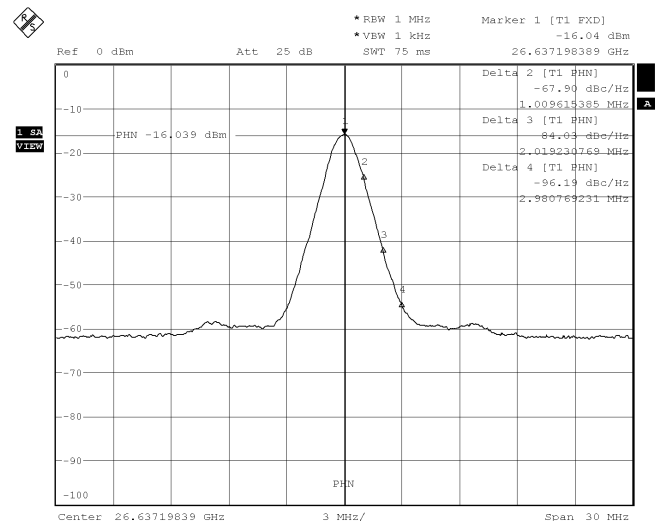


Figure 10.4.6: Measured output spectrum at 26.6GHz.

Continued on Page 596

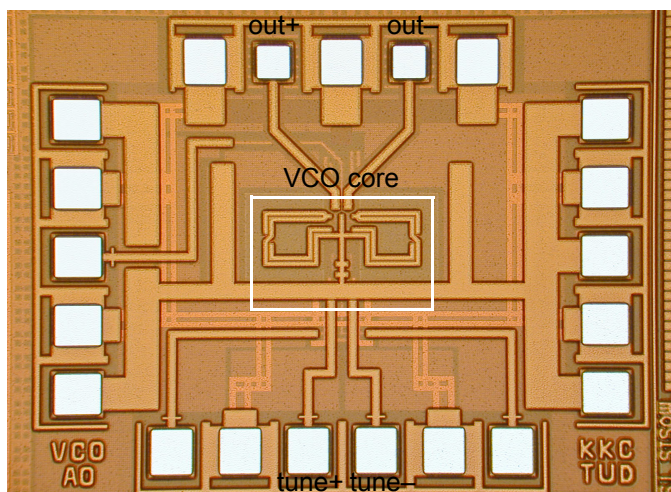


Figure 10.4.7: Transconductance-tuned VCO chip micrograph.